(Received 12 January 2024, Accepted 12 April 2024, Scheduled 21 April 2024)

SAR Flexible Antenna Advancements: Highly Conductive Polymer-Graphene Oxide-Silver Nanocomposites

A. J. A. Al-Gburi[1,*], Mohd M. Ismail[1,*], Naba J. Mohammed[2], and Thamer A. H. Alghamdi[3]

[1] *Center for Telecommunication Research & Innovation (CeTRI), Fakulti Teknologi dan Kejuruteraan Elektronik dan Komputer (FTKEK), Durian Tunggal, Universiti Teknikal Malaysia Melaka (UTeM), Malacca, Malaysia*
[2] *Materials Science Program, Department of Applied Physics, Faculty of Science and Technology University Kebangsaan Malaysia, Bangi 43600, Selangor, Malaysia*
[3] *Wolfson Centre for Magnetics, School of Engineering, Cardiff University, Cardiff CF24 3AA, UK*

ABSTRACT: In the past, copper served as the material for conductive patches in antennas; however, its usage was constrained due to high costs, susceptibility to fading, bulkiness, environmental sensitivity, and manufacturing challenges. The emergence of graphene nanotechnology has positioned graphene as a viable alternative, offering exceptional electrical conductivity, strength, and adaptability. In this study, graphene is employed to fabricate conductive silver nanocomposites. The silver-graphene (Ag/GO) sample exhibits an electrical conductivity of approximately 21.386 S/cm^{-1} as determined by the four-point probe method. The proposed flexible antenna, characterized by four carefully selected cylindrical shapes, is used to construct the antenna patch for enhanced bandwidth and resonates at 2.47 GHz. It achieves remarkable performance characteristics, with a high gain of 11.78 dBi and a return loss greater than −20 dB. Safety considerations are addressed by evaluating the Specific Absorption Rate (SAR). For an input power of 0.5 W, the SAR is calculated to be 1.2 W/kg per 10 g of tissue, affirming the safety of integrating the suggested graphene flexible antenna into flexible devices. In this study, the bending of the antenna was assessed by subjecting the structure to bending at various radii and angles along both the X and Y axes. These findings underscore the promising utility of Ag/GO nanocomposites in the development of flexible antennas for wireless systems.

1. INTRODUCTION

Innovative fabrics and pliable antennas are transforming the landscape of technology and exerting a significant influence across diverse applications [1]. These cutting-edge textiles not only feature visible qualities but also provide intangible capabilities, continuing to save, measure, and modify data and material performance throughout time [2]. Through advancements in textile engineering, these fabrics have acquired the ability to perceive and track various stimuli such as light, touch, sound, and movement. This is accompanied by the capacity for actuation, allowing for the modification of form, light, colour, and warmth [3]. This study investigates the possibility of nanocomposites, specifically those containing silver and graphene oxide (Ag/GO), as a versatile and promising alternative material for such applications. The performance of the material, with a particular focus on conductivity, emerges as a critical factor in determining the abilities of these smart textiles [4]. Silver is unique among metals because of its outstanding electrical and heat conductivity, as well as light reflectance [5]. Despite these advantageous properties, copper and gold are more often used in many applications because of their cost-effectiveness and higher resistance to corrosion [6]. In high-frequency environments, silver may tarnish, leading to a reduction in its conductivity; however, hybridizing it with graphene oxide (GO) provides a viable solution to this issue [7]. Because of its valence configuration and crystalline organisation, silver has the highest electron mobility of any alloy [8]. Other metals with excellent electrical conductivity include aluminium, zinc, nickel, iron, and platinum [9–12]. Interestingly, brass and bronze are conductive alloys rather than pure materials [13, 14]. Graphene oxide's ability to disperse in water and organic solvents makes it a promising material for improving electrical and mechanical properties in matrices [15].

The primary focus is on developing antenna surfaces that can adapt to fabrics, which has prompted the development of novel methods for manufacturing. Conventional techniques such as laser printing [16] and the use of screen printing [17] have created novel approaches to building on-body antenna devices. Unfortunately, the expandability of these approaches in creating flexible antennas is obstructed by the vulnerability of conductive components to corrosion and oxidation. This results in escalated material expenses and a deterioration in performance [18]. Despite grappling with these obstacles, continuous research initiatives persist in investigating a variety of metallic materials, involving conductive copper and silver inks, pleated yarns with Cu/Ag/Au composition, and conductive coatings with Cu/Ag/Au/Al/Ti. The primary aim is to elevate traditional substantial antennas. Unlike many textile substrates, these metallic antennas require particular protection against water absorption and corrosion.

* Corresponding authors: Mohd M. Ismail (muzafar@utem.edu.my) and A. J. A. Al-Gburi (ahmedjamal@ieee.org).

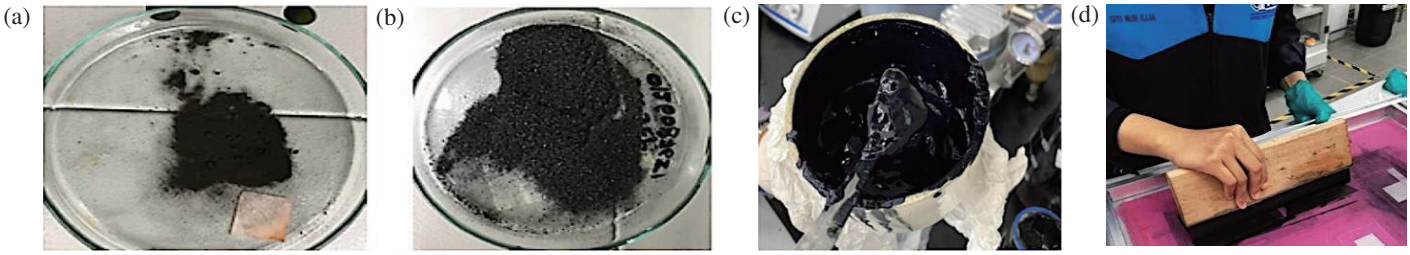

FIGURE 1. Demonstrates the fabrication of Ag/GO nanocomposites: (a) silver powder, (b) graphene powder, (c) rinsed solution, and (d) application on the screen frame using a squeegee at a 45° angle.

Creating efficient and durable wearable antennas in close proximity to the body poses challenges due to the body's high electrical conductivity, resulting in mismatches and losses in the design [19]. The effect of these portable antennas on the human body can be assessed through specific absorption rate (SAR) [20], which measures absorbed power per unit mass, indicating the amount of energy absorbed by biological tissue. SAR serves as a metric for setting human exposure limits and is compared against regulatory standards (such as those established by the FCC and ICNIRP) to ensure safety and prevent harm to individuals [21].

In recent breakthroughs [22], Huang and colleagues have achieved notable progress by ingeniously designing and manufacturing easily printable graphene. This development makes it easier to design transmission lines and antenna systems using paper substrates. A study conducted by AL-Gburi et al. [23] demonstrates the use of highly conductive graphene for wearable antennas. The antenna patch was essentially created through the combination of silver and graphene, resonating at 2.47 GHz. Roy et al. [24] suggested an ultra-wideband flexible antenna for WLAN applications. The antenna was fabricated using a jeans substrate to be operated in on-body conditions. The patch shape is based on a cumulative rugged element fabricated using copper as a conductive sheet. In another study performed by Jaakkola and collaborators [25], screen-printing on Kapton and spray-coating on paper were employed to fabricate dipole antennas incorporating graphene ink and RFID microchips. Nevertheless, the electrical conductivity of both graphene and graphene oxide inks is constrained by interruptions in conductive surfaces caused by lateral size limitations.

This paper describes a novel formulation of graphene oxide and silver particularly intended for wireless communication systems, with a primary emphasis on high conductivity, flexibility, light weight, and cost-effectiveness. Recognising the high conductivity of silver [25] and the good insulating qualities of graphene oxide [26], the study analyses their hybridization to improve electrical conductivity, culminating in a remarkable performance of $21.386 \times 107\,\mathrm{S/m^{-1}}$. Graphene is used in varying amounts to incorporate silver via oxidative aniline polymerization, resulting in the creation of Ag/GO nanocomposites. The quality evaluation includes electrical conductivity tests, morphological exams with Scanning Electron Microscopy (SEM) and Transmission Electron Microscopy (TEM), and conductivity determination in pressed Ag/GO pellets using the four-point probe method. Additionally, Specific Absorption Rate (SAR) values are investigated to address healthcare concerns in flexible devices. The goal of this research is to make a significant contribution to the field of smart textiles and flexible antennas by developing a new material with improved features developed exclusively for wireless communications purposes.

2. CREATION OF A FLEXIBLE ANTENNA BY PREPARING NANOCOMPOSITES OF AG/GO

The preparation process begins with an analysis of raw materials, leading to the formulation of nanocomposites consisting of silver and graphene for flexible textile antennas. Different silver loadings (0.25%, 0.50%, 0.75%, and 1.0%) are utilized as conductive fillers in the graphene nanocomposites. The synthesis of samples at a constant temperature and silver ratio involves the oxidative polymerization of aniline in an acidic medium. Characterization and conductivity tests are carried out to evaluate the effect of graphene concentration on silver conductivity. In this trial, 10.36 grams of aniline hydrochloride and 22.84 grams of ammonium peroxydisulfate are separately immersed in 200 milliliters of distilled water with the aim of producing silver-doped graphene for the creation of a flexible antenna. Following a 12-hour precooling of the solutions at 9°C, they are combined in a beaker. Various concentrations of Ag/GO (0.25 wt%, 0.50 wt%, 0.75 wt%, and 1.0 wt%) are added, and the mixture is stirred for 1 hour with a magnetic stirrer, followed by additional chilling for 24 hours at 9°C.

The obtained mixture undergoes filtration using a 50 kilopascal vacuum filter, followed by washing with 200 milliliters each of 0.2 M hydrochloric acid and acetone (as illustrated in Fig. 1(a)). Subsequently, the filtered material is subjected to drying in a closed-circuit oven for a duration of 24 hours at a temperature of 60 degrees Celsius. Figs. 1(b) and 1(c) showcase the initial powdered forms of silver and graphene before the fusion process. Subsequently, the fabric is laid flat, and Ag/GO ink is applied using a stencil. A squeegee, positioned at a 45° angle, absorbs the ink into the stencil, imprinting the design onto the fabric. Subsequently, the fabric antenna undergoes drying in a microwave at 80 degrees Celsius for a duration of 2 hours (refer to Fig. 1(d)). The flexible antenna geometries are detailed in Fig. 2, where $W = 100$, $L = 70$, $H_s = 0.62$, $R = 15.5$, $F_{le} = 13$, $F_{we} = 43$, $W_f = 1.88$, $L_f = 22.25$ mm.

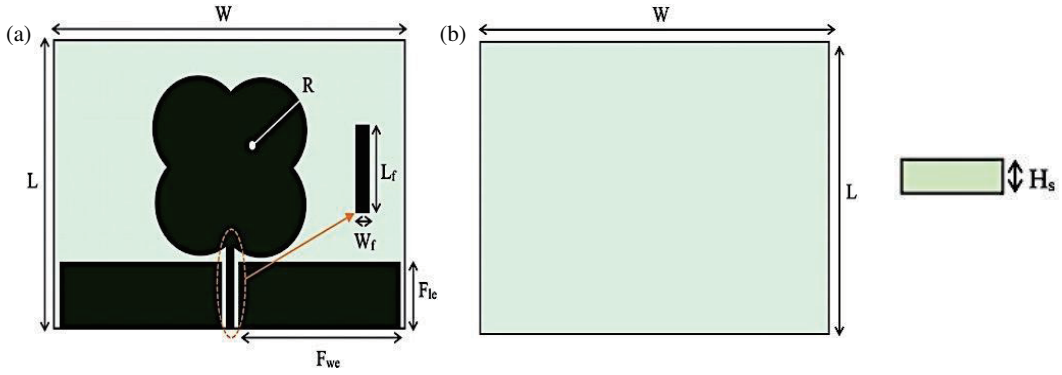

FIGURE 2. The geometry of flexible graphene antenna.

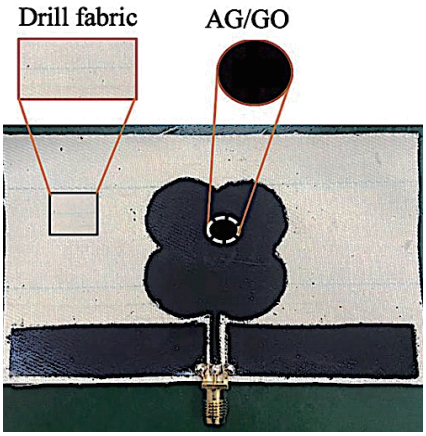

FIGURE 3. Fabricated graphene flexible antenna.

3. RESULTS AND DISCUSSION

The prototype of the fabricated graphene flexible antenna is shown in Fig. 3. SEM at 1000X magnification shows diverse morphologies of Ag/GO particles. Doped silver exhibits different shapes, while graphene oxide appears agglomerated and spherical (Fig. 4(a)). Graphene structure changes post-doping with 0.50 wt% silver, reducing particle aggregation (Fig. 4(b)). Efficient oxidative aniline in situ polymerization at 0.75 wt% and 1.0 wt% silver integrates silver well into the graphene oxide cluster, displaying a flaky morphology (Fig. 4(c)). In situ polymerization demonstrates layer-by-layer diffusion of aniline monomers in graphene nanosheets (Fig. 4(d)). SEM micrographs confirm uniform graphene distribution in Ag/GO nanocomposites. TEM inspection reveals spherical Ag/GO particles with a diameter between 35 and 40 nanometers, as shown in Fig. 4(e).

Silver, existing as an emeraldine salt with partial amorphous and crystalline characteristics, exhibits changes in composite crystallinity reflected in the X-Ray diffraction (XRD) pattern. Ag/GO nanocomposites in Fig. 4(f) show a broad peak at $2\theta = 17.17°$, indicating silver's crystalline structure, with confirmed peaks at $2\theta = 25.65°$ and $26.77°$. Silver concentration, pH, and temperature impact graphene oxide's crystalline structure, showing increased crystallinity post-doping at $2\theta = 26°$. Fourier-transform infrared spectroscopy (FTIR) analysis of Ag/GO nanocomposites (Fig. 4(g)) reveals strong functional group peaks, with vibrational signals at 1600 cm^{-1} and 1400 cm^{-1} identified as $C = C$ bending. The FTIR spectra of pristine Polyaniline (PANI) display recognisable peaks, while silver doping produces novel peaks in Ag/GO, and a slight Van der Waals interaction exists between the graphene oxide and silver.

The flexible antenna demonstrates a -32.6 dB return loss and 740 MHz bandwidth in simulations. Practical measurements at 2.51 GHz show a -20.11 dB return loss with a 713 MHz bandwidth (Fig. 5(a)). Despite a minor frequency shift attributed to substrate permittivity fluctuation, the measured return loss aligns commendably with simulations. Fig. 5(b) shows simulated gain, with the design achieving 11.78 dB at 2.47 GHz. Observations confirm that decreasing permittivity increases flexible gain. The graphene flexible antenna underwent testing in an anechoic chamber, evaluating radiation patterns in the E-plane and H-plane (Fig. 5(c)). The measured E-field pattern closely matches simulations, reflecting high power at that E-field lobe as shown in Fig. 5(d).

The electrical conductivity of Ag/GO nanocomposites was investigated by varying graphene filler loading, measured using a JANDEL model RM3-AR four-point probe for sheet resistance (Fig. 5(e)). Initial pellet pressing yielded 2.80 mm thick discs. The conductivity data for Ag/GO with

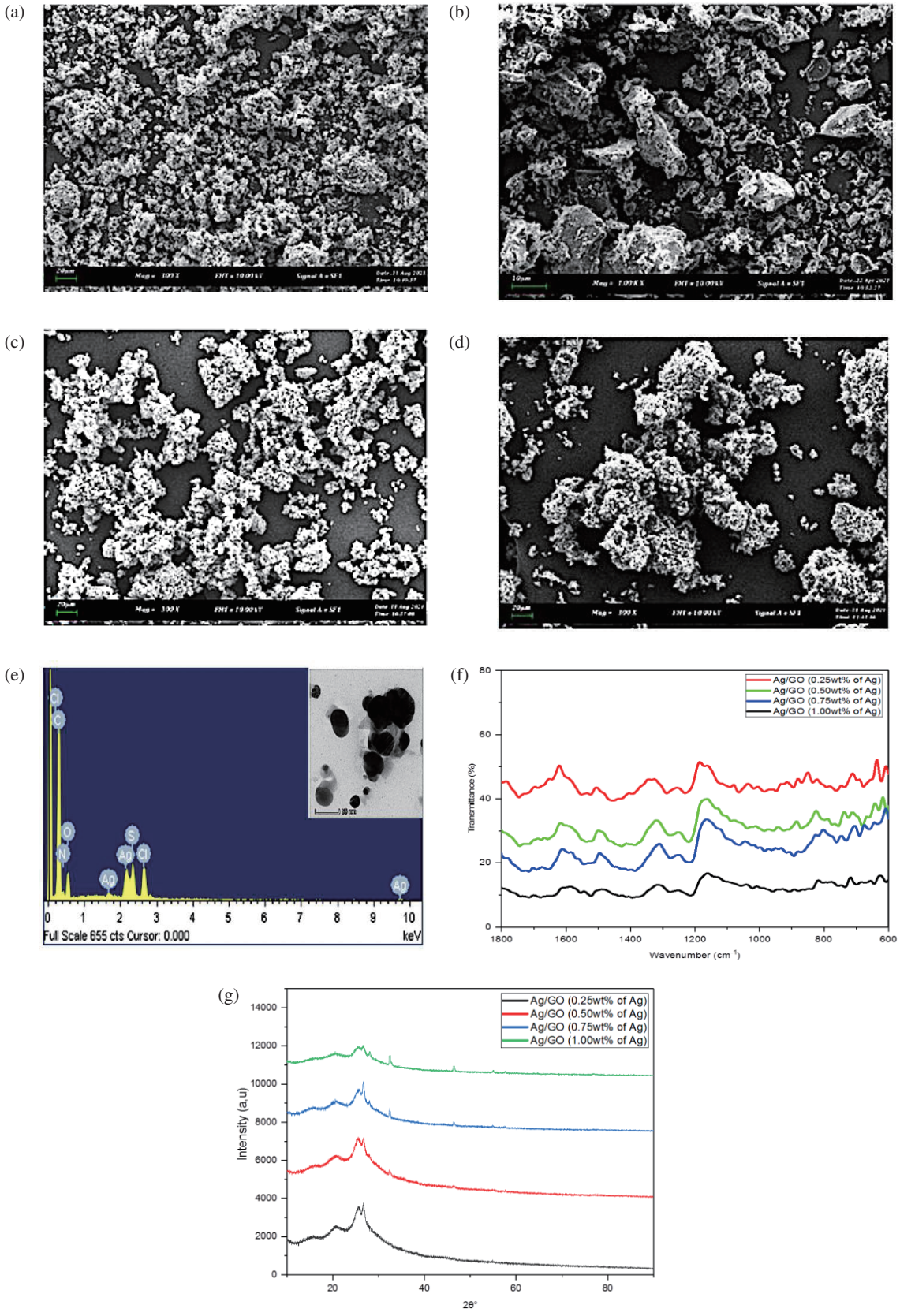

FIGURE 4. SEM analysis with different concentrations (a) at 0.25 wt% silver loadings, (b) at 0.50 wt%, (c) at 0.75 wt%, and (d) at 1.0 wt%, (e) TEM micrograph of Ag/GO with 0.25 wt% silver loadings, (f) XRD patterns for graphene oxide at various concentrations of silver, and (g) FTIR spectra of Ag/GO nanocomposites.

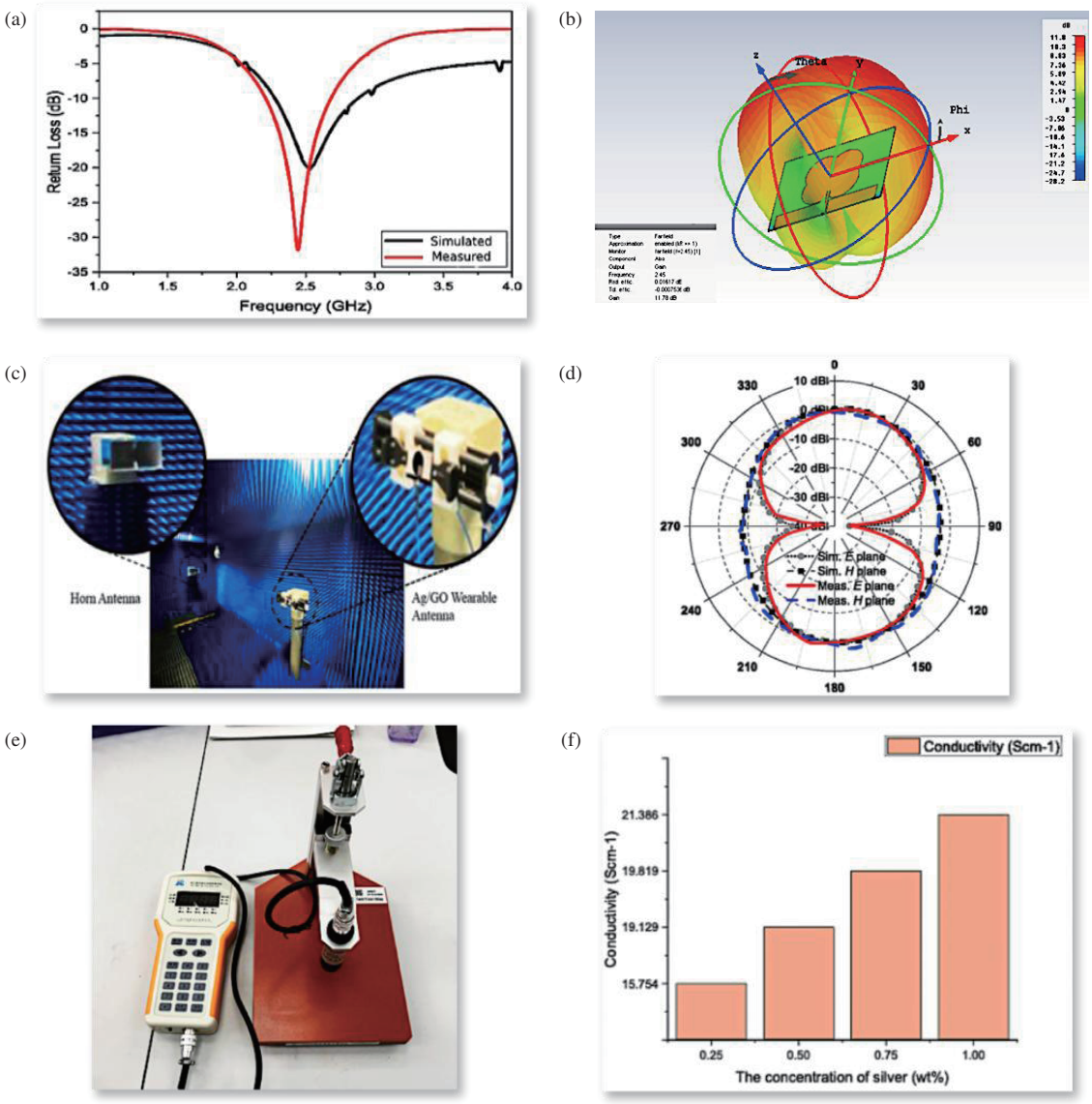

FIGURE 5. Highlights the performance of the flexible graphene antenna across various scenarios, including: (a) a comparison between CST-Simulation and measured return loss, (b) simulation of antenna gain, (c) graphene antenna in an anechoic chamber, (d) a side-by-side assessment of predicted and measured E and H-field patterns, (e) presentation of the actual test equipment for the in-line four-point probe, and (f) exploration of the conductivity of Ag/GO nanocomposites.

0.25 wt%, 0.50 wt%, 0.75 wt%, and 1.00 wt% silver loadings are as follows: 0.25 wt% Ag exhibits a conductivity of 15.754×10^7 Scm^{-1}; 0.50 wt% Ag demonstrates a conductivity of 19.129×10^7 Scm^{-1}; 0.75 wt% Ag displays a conductivity of 19.819×10^7 Scm^{-1}; and 1.00 wt% Ag features a conductivity of 21.386×10^7 Scm^{-1}.

A lower silver concentration (0.25 wt.%) resulted in decreased conductivity compared to pure silver, indicating a disruption in the graphene oxide macromolecular backbone. This disturbance, attributed to the reduced silver concentration, hindered full micelle production during aniline polymerization. Fig. 5(f) depicts the DC conductivity plots, and the collected data are shown in Table 1.

Given the proximity of the intended flexible antenna patch to the body's tissues, particularly the arm, it is essential to evaluate and compare the Specific Absorption Rate (SAR). SAR serves as a crucial metric for assessing radiation exposure. This evaluation must adhere to the specified criteria for assessing electromagnetic radiation as established by both national authorities

TABLE 1. The electrical conductivity measurements were performed on Ag/GO samples with varying silver loadings: 0.25 wt%, 0.50 wt%, 0.75 wt%, and 1.00 wt%.

The degree of substance level of Ag (Wt%)	Conductivity (Scm^{-1})
1.00	21.39×10^7
0.75	19.82×10^7
0.50	19.1×10^7
0.25	15.75×10^7

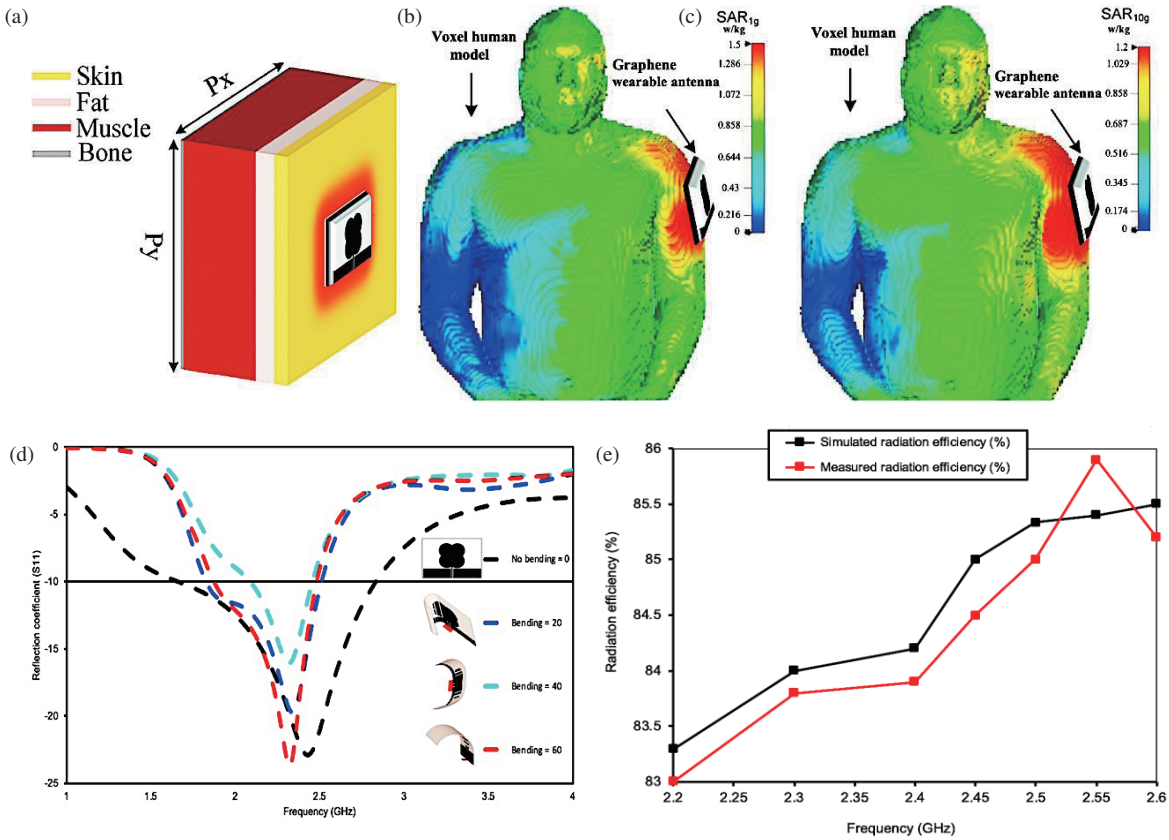

FIGURE 6. Specific Absorption Rate (SAR) and bending analysis in different scenarios: (a) layered phantom model. The visualization of SAR distribution is carried out using the CSTvoxel pattern at 2.47 GHz and 2.5 mm distance from the left arm for (b) SAR1g and (c) SAR10g, and (d) reflection coefficient (S_{11}) bending analysis for different angles (0, 20, 40, and 60 degrees), and (e) simulated and measured radiation antenna efficiency (%).

and IEEE Regulations [27]. Internationally recognized standards, endorsed in the United States and the European Union, outline SAR limitations for the general public: the highest average SAR over the entire body should not exceed 0.08 W/kg; the peak SAR averaged per 1 g of irradiated tissue should not surpass 1.6 W/kg; and the maximum SAR mean within a 10 g tissue volume should be limited to 2 W/kg.

In this investigation, a basic representation of a square composite human arm is employed, and its dimensions are outlined in Table 2. Fig. 6(a) illustrates a straightforward depiction of a human phantom, contrasting it with the intricate multi-layered anatomical voxel model utilized for computing the SAR in this research. The simplified rectangular arm model is deliberately designed to have low complexity, ensuring efficient computational processing with minimal resource requirements. It allows for the adjustment of the quantity, thicknesses, and material properties of tissue layers, resulting in generally precise estimations. In contrast, the anatomical voxel model, which closely approximates the actual composition of the human body, requires substantially more processing resources and time to provide very precise findings. Figs. 6(b) and 6(c) display the SAR distribution from the prototype graphene flexible antenna on the CST-voxel model. SAR values peak near the left arm antenna location, gradually decreasing with distance, consistently remaining below regulatory limits for public safety. In both patch antenna prototypes (Figs. 6(b) and (c)), SAR values remain low consistently, thanks to the presence of a ground-plane layer opposite the patch, facing away from the body. At 0.5 W input power, the lower SAR is 1.2 W/kg at 10 g tissue, and the higher value is 1.5 W/kg at 1 g tissue — Both are within permissible bounds under US and European norms.

Following an analysis of the SAR values of the antenna, confirming its efficacy with minimal SAR and associated impacts on the human body, the antenna's resilience to bending is evaluated through the examination of its S-parameter results. Specifically, the flexibility of graphene antenna is subjected to bending along the X- and Y-axes independently. This assessment aims to ascertain the antenna's functionality under real-world wearable conditions, studying its performance when different sections bend or crumple after being worn.

TABLE 2. Attributes of the model depicting tissues within the human body.

Characteristics of the tissue representation	Skin	Fat	Muscle	Bone
Permittivity	37.9	5.3	52.7	18.5
Conductivity (S/m)	1.5	0.11	1.8	0.8
Density (kg/m^3)	1001	900	1006	1.008
Thickness (mm)	1	5	15	15

The bending of the antenna is defined by its bending radius, denoted as R, as depicted in Fig. 6(d). This study investigates two forms of bending: circular radius bending and angular bending along the X and Y axes. The antenna design in this research employs computer simulation technology (CST) software, with R ranging from 0 mm to 60 mm. It can be clearly seen from Fig. 6(d) that there is a slight shift in the frequency. For example, at 20 mm of bending, the antenna's resonant frequency is 2.3 GHz, and at 40 mm, it is found to be 2.28 GHz. The proposed flexible graphene antenna achieves a high radiation efficiency of approximately 85%, as shown in Fig. 6(e).

4. CONCLUSIONS

In this brief, the constraints associated with the use of copper in antennas, including cost, vulnerability to multipath fading, unwieldiness, environmental issues, and manufacturing intricacies, have prompted a search for alternative materials. This paper recommends using graphene as an appropriate replacement for copper in antenna design, leveraging its extraordinary electrical conductivity, greater strength, versatility, and flexibility. The focus is on incorporating graphene into silver nanocomposites (Ag/GO). The resulting samples had high electrical conductivity, at 21.386 S/cm, demonstrating graphene's efficiency in enhancing material conductivity. The practical application is demonstrated by designing and assembling a flexible antenna with a circular patch and strategically placed slots to increase impedance bandwidth. This flexible antenna achieves resonance at 2.47 GHz, demonstrating excellent performance parameters such as high gain of 11.78 dBi and return loss greater than -20 dB. Additionally, the study addresses health considerations by conducting Specific Absorption Rate (SAR) assessments for wearable devices, demonstrating a potential use of silver-graphene nanocomposites in flexible antennas for wireless communication devices. This highlights the enhanced electrical conductivity, flexibility, and versatility of graphene, contributing to the progression of more effective and adaptable wearable communication systems. Not only does this research surpass previous material constraints, but it also establishes a foundation for future advancements in antenna technology applicable to various wireless communication scenarios.

ACKNOWLEDGEMENT

The authors express their thank and acknowledge the support from Universiti Teknikal Malaysia Melaka (UTeM), the Centre for Research and Innovation Management (CRIM), and the Ministry of Higher Education of Malaysia (MOHE).

REFERENCES

[1] Ibanez-Labiano, I., M. S. Ergoktas, C. Kocabas, A. Toomey, A. Alomainy, and E. Ozden-Yenigun, "Graphene-based soft wearable antennas," *Applied Materials Today*, Vol. 20, 100727, Sep. 2020.

[2] Hasni, U., M. E. Piper, J. Lundquist, and E. Topsakal, "Screen-printed fabric antennas for wearable applications," *IEEE Open Journal of Antennas and Propagation*, Vol. 2, 591–598, 2021.

[3] Saunders, S. R. and A. Aragón-Zavala, *Antennas and Propagation for Wireless Communication Systems*, John Wiley & Sons, 2007.

[4] Le, T. T., Y.-D. Kim, and T.-Y. Yun, "A triple-band dual-open-ring high-gain high-efficiency antenna for wearable applications," *IEEE Access*, Vol. 9, 118 435–118 442, 2021.

[5] Karim, N., S. Afroj, S. Tan, K. S. Novoselov, and S. G. Yeates, "All inkjet-printed graphene-silver composite ink on textiles for highly conductive wearable electronics applications," *Scientific Reports*, Vol. 9, No. 1, 8035, 2019.

[6] Abu-Hamdeh, N. H., E. Almatrafi, M. Hekmatifar, D. Toghraie, and A. Golmohammadzadeh, "Molecular dynamics simulation of the thermal properties of the cu-water nanofluid on a roughed platinum surface: simulation of phase transition in nanofluids," *Journal of Molecular Liquids*, Vol. 327, 114832, 2021.

[7] Olabi, A. G., M. A. Abdelkareem, T. Wilberforce, and E. T. Sayed, "Application of graphene in energy storage device — A review," *Renewable and Sustainable Energy Reviews*, Vol. 135, 110026, 2021.

[8] Karim, N., S. Afroj, A. Malandraki, S. Butterworth, C. Beach, M. Rigout, K. S. Novoselov, A. J. Casson, and S. G. Yeates, "All inkjet-printed graphene-based conductive patterns for wearable e-textile applications," *Journal of Materials Chemistry C*, Vol. 5, No. 44, 11 640–11 648, 2017.

[9] Wang, L., X. Kong, J. Ren, M. Fan, and H. Li, "Novel hybrid composite phase change materials with high thermal performance based on aluminium nitride and nanocapsules," *Energy*, Vol. 238, 121775, 2022.

[10] Moghaddam, A. R., Z. Ranjbar, U. Sundararaj, A. Jannesari, and M. Kamkar, "A novel electrically conductive water borne epoxy nanocomposite coating based on graphene: Facile method and high efficient graphene dispersion," *Progress in Organic Coatings*, Vol. 136, 105223, 2019.

[11] Vinnik, D. A., V. E. Zhivulin, D. P. Sherstyuk, A. Y. Starikov, P. A. Zezyulina, S. A. Gudkova, D. A. Zherebtsov, K. N. Rozanov, S. V. Trukhanov, K. A. Astapovich, *et al.*, "Electromagnetic properties of zinc–nickel ferrites in the frequency range of 0.05–10 GHz," *Materials Today Chemistry*, Vol. 20, 100460, 2021.

[12] Zhao, J., K. Ni, Y. Su, and Y. Shi, "An evaluation of iron ore tailings characteristics and iron ore tailings concrete properties," *Construction and Building Materials*, Vol. 286, 122968, 2021.

[13] Weinreich, J., M. L. Paleico, and J. Behler, "Properties of α-brass nanoparticles II: Structure and composition," *The Journal of Physical Chemistry C*, Vol. 125, No. 27, 14 897–14 909, 2021.

[14] Senatore, A., G. Risitano, L. Scappaticci, and D. D'Andrea, "Investigation of the tribological properties of different textured lead bronze coatings under severe load conditions," *Lubricants*, Vol. 9, No. 4, 34, 2021.

[15] Saeidi, T., A. J. A. Al-Gburi, and S. Karamzadeh, "A miniaturized full-ground dual-band MIMO spiral button wearable antenna for 5G and sub-6 GHz communications," *Sensors*, Vol. 23, No. 4, 1997, 2023.

[16] Whittow, W. G., A. Chauraya, J. C. Vardaxoglou, Y. Li, R. Torah, K. Yang, S. Beeby, and J. Tudor, "Inkjet-printed microstrip patch antennas realized on textile for wearable applications," *IEEE Antennas and Wireless Propagation Letters*, Vol. 13, 71–74, 2014.

[17] Scarpello, M. L., I. Kazani, C. Hertleer, H. Rogier, and D. V. Ginste, "Stability and efficiency of screen-printed wearable and washable antennas," *IEEE Antennas and Wireless Propagation Letters*, Vol. 11, 838–841, 2012.

[18] Zhang, J., G. Y. Tian, A. M. J. Marindra, A. I. Sunny, and A. B. Zhao, "A review of passive RFID tag antenna-based sensors and

systems for structural health monitoring applications," *Sensors*, Vol. 17, No. 2, 265, 2017.

[19] Ahmad, S., H. Boubakar, S. Naseer, M. E. Alim, Y. A. Sheikh, A. Ghaffar, A. J. A. Al-Gburi, and N. O. Parchin, "Design of a tri-band wearable antenna for millimeter-wave 5G applications," *Sensors*, Vol. 22, No. 20, 8012, Oct. 2022.

[20] Butt, A. D., J. Khan, S. Ahmad, A. Ghaffar, A. J. A. Al-Gburi, and M. Hussein, "Single-fed broadband CPW-fed circularly polarized implantable antenna for sensing medical applications," *Plos One*, Vol. 18, No. 4, e0280042, 2023.

[21] Elabd, R. H. and A. J. A. Al-Gburi, "SAR assessment of miniaturized wideband MIMO antenna structure for millimeter wave 5G smartphones," *Microelectronic Engineering*, Vol. 282, 112098, 2023.

[22] Huang, X., T. Leng, M. Zhu, X. Zhang, J. Chen, K. Chang, M. Aqeeli, A. K. Geim, K. S. Novoselov, and Z. Hu, "Highly flexible and conductive printed graphene for wireless wearable communications applications," *Scientific Reports*, Vol. 5, No. 1, 1–8, 2016.

[23] Al-Gburi, A. J. A., M. M. Ismail, N. J. Mohammed, A. Buragohain, and K. Alhassoon, "Electrical conductivity and morphological observation of hybrid filler: Silver-graphene oxide nanocomposites for wearable antenna," *Optical Materials*, Vol. 148, 114882, 2024.

[24] Roy, A., A. K. Biswas, A. Nandi, and B. Basu, "Ultra-wideband flexible wearable antenna with notch characteristics for WLAN applications," *Progress In Electromagnetics Research C*, Vol. 129, 143–155, 2023.

[25] Jaakkola, K., V. Ermolov, P. G. Karagiannidis, S. A. Hodge, L. Lombardi, X. Zhang, R. Grenman, H. Sandberg, A. Lombardo, and A. C. Ferrari, "Screen-printed and spray coated graphene-based RFID transponders," *2D Materials*, Vol. 7, No. 1, 015019, 2019.

[26] Xu, L. Y., G. Y. Yang, H. Y. Jing, J. Wei, and Y. D. Han, "Ag-graphene hybrid conductive ink for writing electronics," *Nanotechnology*, Vol. 25, No. 5, 055201, 2014.

[27] IEC/IEEE International Standard, "Determining the peak spatial-average specific absorption rate (SAR) in the human body from wireless communications devices, 30 MHz to 6 GHz-part 1: General requirements for using the finite-difference time-domain (FDTD) method for SAR calculations," IEC/IEEE 62704-1:2017, IEEE, Piscataway, NJ, USA, 2017.